Am J Physiol Lung Cell Mol Physiol 300: L548–L559, 2011.
First published January 28, 2010; doi:10.1152/ajplung.00230.2010.

Interplay between RAGE, CD44, and focal adhesion molecules in epithelial-mesenchymal transition of alveolar epithelial cells

Stephen T. Buckley,[1] Carlos Medina,[1] Michael Kasper,[2] and Carsten Ehrhardt[1]

[1]*School of Pharmacy and Pharmaceutical Sciences, Trinity College Dublin, Dublin, Ireland; and* [2]*Institute of Anatomy, Technical University of Dresden, Dresden, Germany*

Submitted 8 July 2010; accepted in final form 19 January 2011

Buckley ST, Medina C, Kasper M, Ehrhardt C. Interplay between RAGE, CD44, and focal adhesion molecules in epithelial-mesenchymal transition of alveolar epithelial cells. *Am J Physiol Lung Cell Mol Physiol* 300: L548–L559, 2011. First published January 28, 2010; doi:10.1152/ajplung.00230.2010.—Fibrosis of the lung is characterized by the accumulation of myofibroblasts, a key mediator in the fibrogenic reaction. Cumulative evidence indicates that epithelial-mesenchymal transition (EMT), a process whereby epithelial cells become mesenchyme-like, is an important contributing source for the myofibroblast population. Underlying this phenotypical change is a dramatic alteration in cellular structure. The receptor for advanced glycation end-products (RAGE) has been suggested to maintain lung homeostasis by mediating cell adhesion, while the family of ezrin/radixin/moesin (ERM) proteins, on the other hand, serve as an important cross-linker between the plasma membrane and cytoskeleton. In the present investigation, we tested the hypothesis that RAGE and ERM interact and play a key role in regulating EMT-associated structural changes in alveolar epithelial cells. Exposure of A549 cells to inflammatory cytokines resulted in phosphorylation and redistribution of ERM to the cell periphery and localization with EMT-related actin stress fibers. Simultaneously, blockade of Rho kinase (ROCK) signaling attenuated these cytokine-induced structural changes. Additionally, RAGE expression was diminished after cytokine stimulation, with release of its soluble isoform via a matrix metalloproteinase (MMP)-9-dependent mechanism. Immunofluorescence microscopy and coimmunoprecipitation revealed association between ERM and RAGE under basal conditions, which was disrupted when challenged with inflammatory cytokines, as ERM in its activated state complexed with membrane-linked CD44. Dual-fluorescence immunohistochemistry of patient idiopathic pulmonary fibrosis (IPF) tissues highlighted marked diminution of RAGE in fibrotic samples, together with enhanced levels of CD44 and double-positive cells for CD44 and phospho (p)ERM. These data suggest that dysregulation of the ERM-RAGE complex might be an important step in rearrangement of the actin cytoskeleton during proinflammatory cytokine-induced EMT of human alveolar epithelial cells.

fibrosis; ezrin/radixin/moesin; transdifferentiation; cytoskeleton

IDIOPATHIC PULMONARY FIBROSIS (IPF) is characterized by a marked disruption in the integrity and structure of the alveolar epithelium. Specifically, injury to the alveolar epithelium gives rise to delayed reepithelialization, leading to a denuded, disrupted basement membrane (41). In light of their compromised capacity to reestablish a physiological epithelial lining, increasing evidence suggests that affected populations of alveolar epithelial cells may undergo epithelial-mesenchymal transition (EMT), and in this way serve as a source of pathogenic mesenchymal cell types (44, 45). Core to this process is the cytoskeletal rearrangement of their actin structures. After induction of EMT by proinflammatory cytokines [e.g., transforming growth factor (TGF)-β1, TNF-α, IL-1β], actin filament architecture changes dynamically from a cortical actin network to stress fibers (18). Although currently very little is known about the mechanisms that underlie these structural rearrangements, conceivably a better insight into these mechanisms may provide novel targets or approaches to ameliorate or prevent EMT-related structural alterations of the alveolus in IPF.

The ezrin/radixin/moesin (ERM) family of proteins provide a regulated linkage from the filamentous (F-)actin to membrane proteins on the surface of cells (24). In their native state they remain in a folded conformation due to an intramolecular interaction between their NH_2- and COOH-terminal domains, which masks the membrane and F-actin binding sites. Upon phosphorylation, ERM proteins become activated, enabling interaction with integral membrane proteins (e.g., CD44) and F-actin. Cumulative research suggests that proteins of the ERM family play a crucial functional role in regulating cell shape (10). Notably, in a *Drosophila*-based model of epithelia altered expression of ERM proteins resulted in disruption of epithelial morphology and integrity, with cells exhibiting a more invasive migratory pattern (36). Moreover, while their exact function in pulmonary physiology remains poorly characterized, a recent study suggests that ERM proteins may play a key role in the regulation of alveolar structure and lung homeostasis (14).

The receptor for advanced glycation end-products (RAGE) is a member of the immunoglobulin superfamily (27). Uniquely, it is expressed at extremely high levels in the lung under physiological conditions, whereas in most other organs low baseline RAGE levels can be observed, which increase during various pathologies such as diabetes, inflammation, and cancer (3). Previously, our laboratory showed (8) that RAGE plays an important role in alveolar epithelial cell function, facilitating cell spreading and adherence. Its importance is further emphasized by the fact that impairment of RAGE signaling gives rise to enhanced cell migration and proliferation (30). Additionally, RAGE appears to be linked to cytoskeletal components within pulmonary epithelial cells (8, 30) and, in this way, may mediate its regulatory adhesion function. From these observations, RAGE has been concluded to be involved in the maintenance of lung homeostasis. In particular, this has been highlighted in pathological settings, in which loss of RAGE has been associated with a fibrotic response (9, 30).

In this work, we tested the hypothesis that both ERM and RAGE serve as important regulators in the maintenance of normal alveolar epithelial structure and function, and that disruption of their basal expression patterns may be an impor-

Address for reprint requests and other correspondence: C. Ehrhardt, School of Pharmacy and Pharmaceutical Sciences, Trinity College Dublin, Panoz Inst., Dublin 2, Ireland (e-mail: ehrhardc@tcd.ie).

tant feature of alveolar EMT. Our findings revealed an association between ERM and RAGE in the A549 human alveolar epithelial cell line. Cytokine stimulation elicited a dramatic reorganization of ERM toward the cell periphery that was attenuated by Rho kinase (ROCK). In tandem, proteolytic cleavage of RAGE by matrix metalloproteinase (MMP)-9 was observed. Additionally, we observed interactions between newly formed actin stress fibers and ERM proteins. Taken together, these data suggest that dysregulation of the ERM-RAGE complex might be a key event in actin microfilament rearrangement during cytokine-induced alveolar EMT.

MATERIALS AND METHODS

Materials. Goat polyclonal anti-RAGE antibody and rabbit monoclonal anti-MMP-9 antibody were purchased from Millipore (Carrigtwohill, Ireland). Rabbit polyclonal anti-ERM antibody and anti-phospho (p)ERM antibody and mouse monoclonal anti-CD44 antibody were purchased from Cell Signaling (Danvers, MA). Tetramethylrhodamine isothiocyanate (TRITC)-phalloidin was purchased from Sigma-Aldrich (Dublin, Ireland). Recombinant human TGF-β1, IL-1β, TNF-α, and IFN-γ were purchased from PeproTech (London, UK). Cell culture medium, fetal bovine serum (FBS), and all other reagents were purchased from Sigma-Aldrich.

Cell culture conditions. A549 human alveolar epithelial cells [American Type Culture Collection (ATCC) CL-185] were obtained from the European Collection of Animal Cell Cultures (ECACC, Salisbury, UK) and used between *passages 65* and *89*. Cells were maintained in a 1:1 mixture of Dulbecco's modified Eagle's medium and Ham's nutrient mixture F-12 medium (DMEM-F-12) supplemented with 5% (vol/vol) FBS, 100 U/ml penicillin, and 100 μg/ml streptomycin. Cells were cultured at 37°C in a 5% CO_2 atmosphere, and culture medium was exchanged every 48 h. For studies described below, after 1 day in culture cells were serum-starved overnight and then treated with TGF-β1 (5 ng/ml) and/or cytomix (10 ng/ml TNF-α, 10 ng/ml IL-1β, 10 ng/ml IFN-γ) in culture medium containing 1% FBS for 72 h as previously described (4). In those experiments using either Y-27632 (Sigma-Aldrich) or MMP-9 Inhibitor I (Calbiochem, San Diego, CA), cells were preincubated for 2 h before cytokine stimulation. In the case of recombinant MMP-9 treatments, cells were incubated for 72 h in medium containing 1% FBS.

Western blot analysis. Cell cultures were lysed with cell extraction buffer (Invitrogen, Karlsruhe, Germany) on ice and briefly sonicated. In the case of cell supernatants, culture medium was removed after treatments as detailed above. Protein sample concentrations were determined by a standard protein concentration assay (Bio-Rad, Hemel Hempstead, UK) according to the manufacturer's instructions. Samples were separated by sodium dodecyl sulfate-polyacrylamide gel electrophoresis (SDS-PAGE) and transferred to immunoblot polyvinylidene fluoride membranes (Bio-Rad). Membranes were blocked in 5% bovine serum albumin (BSA) in Tris-buffered saline with Tween 20 (pH 7.4) for 1 h at room temperature. Incubation with the respective primary antibody was carried out overnight at 4°C, followed by incubation with horseradish peroxidase (HRP)-conjugated secondary antibody at room temperature for 1 h. Peroxidase activity was detected with Immobilon Western Chemiluminescent HRP substrate (Millipore). Relative levels of protein expression were quantified by densitometric analysis of the immunoblot with a ChemiDoc documentation system (Bio-Rad). When appropriate, blots were stripped and analyzed for β-actin (Sigma-Aldrich) as internal control and total ERM.

Immunofluorescence microscopy. Lab-Tek chamber slides (Nunc, Roskilde, Denmark) were used to grow A549 cells under conditions as described above. Cells were fixed for 10 min with 2% (wt/vol) paraformaldehyde and incubated for 10 min in 50 mM NH_4Cl, followed by permeabilization for 8 min with 0.1% (wt/vol) Triton X-100 in PBS. After a 60-min incubation with 150 μl of dilution [CD44 1:100, ERM 1:100, pERM 1:100, RAGE 1:300, MMP-9 1:100] of the respective primary antibody, the cell layers were washed three times with PBS before incubation with 100 μl of a 1:200 dilution of relevant Alexa Fluor-labeled $F(ab')_2$ fragment (Invitrogen) in PBS containing 1% (wt/vol) BSA. Propidium iodide (1 μg/ml in PBS) was used to counterstain cell nuclei. In the case of F-actin staining, TRITC-phalloidin was used at a concentration of 500 ng/ml in PBS. After 30 min of incubation, the specimens were again washed three times with PBS and embedded in FluorSave antifade medium (Merck, Nottingham, UK). Images were obtained with a confocal laser scanning microscope (CLSM; Zeiss LSM 510, Göttingen, Germany), with the instrument's settings adjusted so that no positive signal was observed in the channel corresponding to the fluorescence of the isotypic controls.

Gelatin zymography. Gelatinase activity (MMP-2 and -9) was measured in A549 cell-conditioned medium as previously described (26). Samples were subjected to 10% SDS-PAGE with copolymerized 0.2% (wt/vol) gelatin. After electrophoresis, the gels were washed twice for 20 min each with 2% (wt/vol) Triton X-100 and then incubated in development buffer (in mmol: 50 Tris·HCl, 200 NaCl, 10 $CaCl_2$ and 1 $ZnCl_2$; pH 7.5) at 37°C overnight for the development of enzyme activity bands. Conditioned medium of HT-1080 human fibrosarcoma cells, which contains high amounts of both MMP-2 and -9, was used as standard. After incubation, gels were fixed and stained in 40% methanol, 10% acetic acid, and 0.1% (wt/vol) Coomassie brilliant blue for 1 h and then destained. The gelatinolytic activities were detected as transparent bands against the background of Coomassie brilliant blue-stained gelatin. Images were analyzed with a ChemiDoc documentation system (Bio-Rad).

Coimmunoprecipitation. Two hundred microliters of lysate from A549 cells grown as described above was added to prewashed protein A/G beads (20 μl of 50% bead slurry; Sigma-Aldrich) and incubated at 4°C for 60 min. The mixture was then centrifuged for 10 min at 4°C. Next, the supernatant was incubated with goat antibody against RAGE or CD44 at 4°C overnight. Prewashed protein A/G beads (20 μl at 50%) were then added to the mixture and incubated for 3 h at 4°C. After centrifugation, beads were washed five times with solubilization buffer (in mM: 20 Tris·HCl pH 7.4, 5 EDTA, and 150 NaCl, with 10% glycerol and 1% Triton X-100). Isolated protein complexes were denatured for 5 min at 95°C, analyzed by gel electrophoresis, and transferred to polyvinyl difluoride (PVDF) membranes, followed by immunoblotting with anti-ERM or anti-pERM antibodies and detection with Immobilon Western Chemiluminescent HRP substrate. The purity of each immunoprecipitation complex was verified by reblotting for β-actin.

Immunohistochemistry. The following antibodies were used: mouse monoclonal anti-human antibody clone 11.24 against a CD44v9 epitope used as hybridoma supernatant (kind gift from Dr. U. Günthert, University of Basel, Institute of Pathology, Basel, Switzerland), diluted 1:10; goat polyclonal anti-RAGE (kind gift from Dr. Michael Neeper, Merck Sharp & Dohme, West Point, PA), diluted 1:1,000; and rabbit polyclonal anti-pERM (Cell Signaling), diluted 1:50. Retrospective tissue samples taken from a previous study (46) were used. For double immunofluorescence, paraffin sections were incubated with primary antibodies followed by incubation with goat anti-mouse immunoglobulin (IgG), FITC coupled (dilution 1:80, Dianova, Hamburg, Germany), or goat anti-rabbit IgG, Texas Red labeled (dilution 1:80, Dianova). As negative controls the primary antibodies were replaced with PBS or nonimmune IgG.

Statistical analysis. Results are expressed as means ± SD compared by one-way analysis of variance (ANOVA) followed by the Student-Newman-Keuls post hoc test. $P < 0.05$ was considered significant.

RESULTS

ERM proteins undergo redistribution and activation after exposure to TGF-β1 and/or cytomix and colocalize with actin stress fibers. Under basal conditions, ERM proteins exhibited a predominantly cytoplasmic distribution in A549 cells (Fig. 1*A*). After treatment with TGF-β1 and/or cytomix, a marked redistribution of ERM toward the plasmalemma was observed (Fig. 1, *B–D*). This was coupled with alterations in cell morphology, with cells adopting a fibroblast-like shape. In tandem, immunoblot analysis revealed that cytokine treatment induced activation of ERM proteins, as evidenced by their phosphorylation (Fig. 1*E*). To explore their involvement in EMT-associated cytoskeletal rearrangement, colocalization studies were performed by CLSM. In untreated cells, actin was strongly associated with the adherens junctions (Fig. 1*F*), whereas stimulation with TGF-β1 and/or cytomix resulted in reorganization of cortical filaments, with cells exhibiting elongated stress fibers similar to those found in fibroblasts. Notably, ERM proteins were found to strongly colocalize with these newly formed F-actin fibers (Fig. 1, *G–I*).

Effect of ROCK inhibition on ERM phosphorylation and actin stress fiber formation. To determine the signaling pathway through which proinflammatory cytokines activate ERM, A549 cells were incubated with Y-27632, a specific inhibitor of ROCK, followed by treatment with TGF-β1, cytomix, or both. As observed by Western blot, inhibition of ROCK signaling prevented ERM phosphorylation (Fig. 2*A*). Its effect was most apparent in cells treated with TGF-β1 in the presence or absence of cytomix, while less so in those stimulated by cytomix alone. This suggests that phosphorylation of ERM mediated by proinflammatory cytokines is primarily mediated via a ROCK-dependent pathway. Of note, morphological anal-

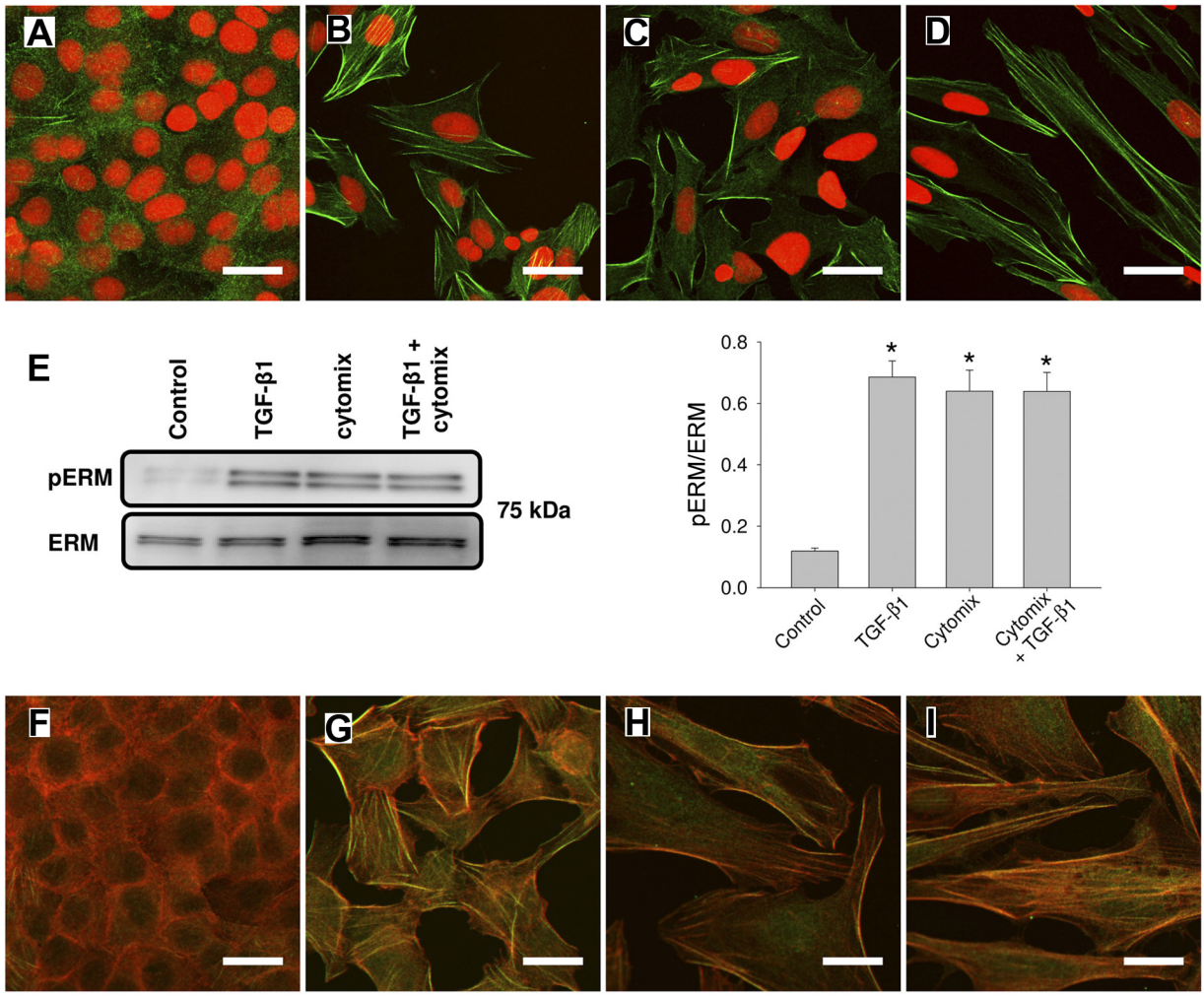

Fig. 1. *A–D*: redistribution and activation of ezrin/moesin/radixin (ERM) proteins following stimulation with transforming growth factor (TGF)-β1 and/or cytomix and colocalization with actin stress fibers; immunofluorescence staining for ERM (green). *A*: untreated A549 cells. *B–D*: A549 cells were grown on chamber slides and stimulated with TGF-β1 (5 ng/ml; *B*), cytomix (10 ng/ml; *C*), or TGF-β1 + cytomix (*D*) for 72 h. Nuclei were counterstained with propidium iodide (red). Treatment of A549 cells gave rise to marked redistribution of ERM from the cytoplasm to the cell periphery. *E*: Western blot analysis of cell lysates for phospho (p)ERM. Treatment of A549 cells with TGF-β1 and/or cytomix induced phosphorylation of ERM proteins. Expression levels were evaluated by densitometric analysis and standardized by comparison to total ERM. *F–I*: for visualization of F-actin, A549 cells were fixed and labeled with tetramethylrhodamine isothiocyanate (TRITC)-phalloidin (red). *F*: untreated cells. After treatment with TGF-β1 (5 ng/ml; *G*), cytomix (10 ng/ml; *H*), or TGF-β1 + cytomix (*I*), A549 cells acquired a more fibroblast-like morphology together with formation of F-actin stress fibers. ERM proteins (green) exhibited strong colocalization with these newly formed stress fibers. Means ± SD from >3 independent experiments. *$P < 0.05$. Scale bars are 20 μm.

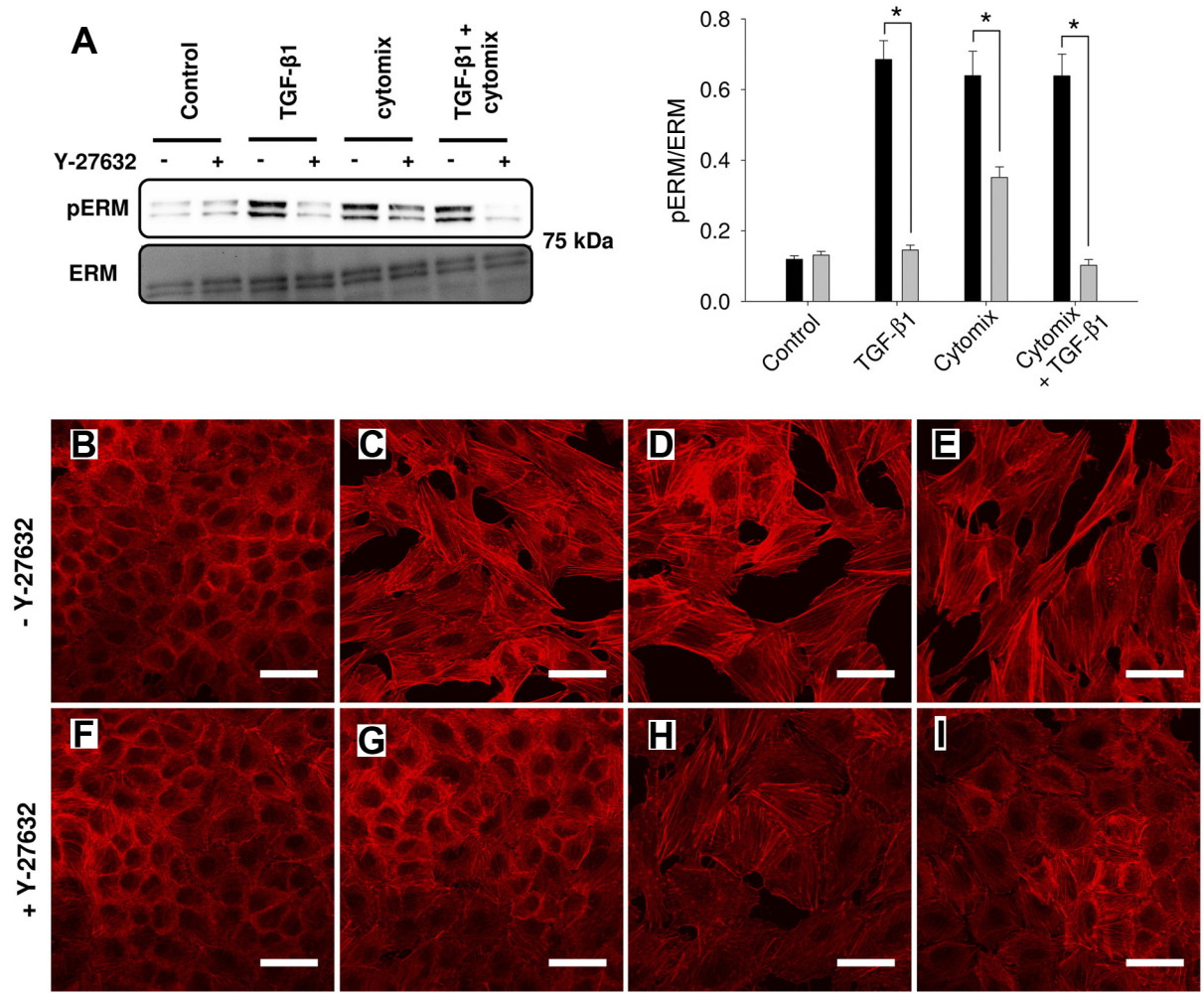

Fig. 2. Rho kinase (ROCK)-dependent phosphorylation of ERM proteins and actin stress fiber formation. A549 cells were incubated with Y-27632 (5 μM), a specific inhibitor of ROCK, followed by treatment with TGF-β1, cytomix, or TGF-β1 + cytomix for 72 h. *A*: Western blot analysis revealed that cytokine-induced ERM phosphorylation was blocked after inhibition of ROCK signaling. pERM, phospho-ERM. *B–I*: F-actin structures were visualized with TRITC-phalloidin and examined by confocal laser scanning microscopy (CLSM). *B* and *F*: untreated. *C* and *G*: TGF-β1. *D* and *H*: cytomix. *E* and *I*: TGF-β1 + cytomix. Preincubation with Y-27632 ensured maintenance of cortical actin architectures in cells stimulated with TGF-β1 (*G*), while in those treated with either cytomix (*H*) or TGF-β1 + cytomix (*I*) the incidence of stress fiber formation was notably diminished. Means ± SD from >3 independent experiments. *$P < 0.05$.

ysis using phalloidin staining revealed that exposure to ROCK inhibitor Y-27632 prevented formation of mesenchyme-associated actin stress fibers in those cells stimulated with TGF-β1 while reducing stress fiber numbers in cytomix- and TGF-β1 plus cytomix-treated cells (Fig. 2, *B–I*).

RAGE is downregulated and released in its soluble form when challenged by proinflammatory cytokines. We have previously shown (8) that RAGE associates with intermediate filaments and microfilaments of the cytoskeleton. Given this finding, we investigated its expression following cytokine-induced remodeling of the cytoskeleton. Western blot analysis revealed abundant expression of RAGE in alveolar epithelial (A549) cells (Fig. 3*A*), with immunofluorescence microscopy indicating that it was localized to the membrane as well as the cytoplasm (Fig. 3, *B–E*). Exposure to TGF-β1 and, to a greater extent, cytomix plus TGF-β1 and cytomix alone resulted in a marked diminution of RAGE expression (Fig. 3, *A–E*).

RAGE exists in a number of different isoforms (3, 12). We hypothesized that RAGE may be cleaved, giving rise to release of its soluble isoform, sRAGE. With Western blot, the level of RAGE in cell medium was assessed. Investigations revealed that RAGE levels in cytokine-stimulated medium were significantly higher than those in medium from control cells (Fig. 3*F*).

Release of sRAGE is mediated by MMP-9. Next, we determined the mechanism for release of sRAGE. MMPs are known to be upregulated in fibrotic disorders of the lung, actively contributing to tissue remodeling (1). Specifically, MMP-9 is a known mediator of alveolar basement membrane disruption (28) and has been previously implicated in protein ectodomain shedding (25). In light of this, we investigated whether proteolytic cleavage of RAGE was mediated by MMP-9.

In A549 cells pretreated with MMP-9 Inhibitor I, a selective inhibitor of MMP-9, before cytokine stimulation there was a marked decrease of RAGE in cell supernatants (Fig. 4*A*). Using gelatin zymography, we verified that treatment with TGF-β1 and/or cytomix enhanced MMP-9 activity. MMP-2, however, remained unchanged (Fig. 4*B*). In agreement with these find-

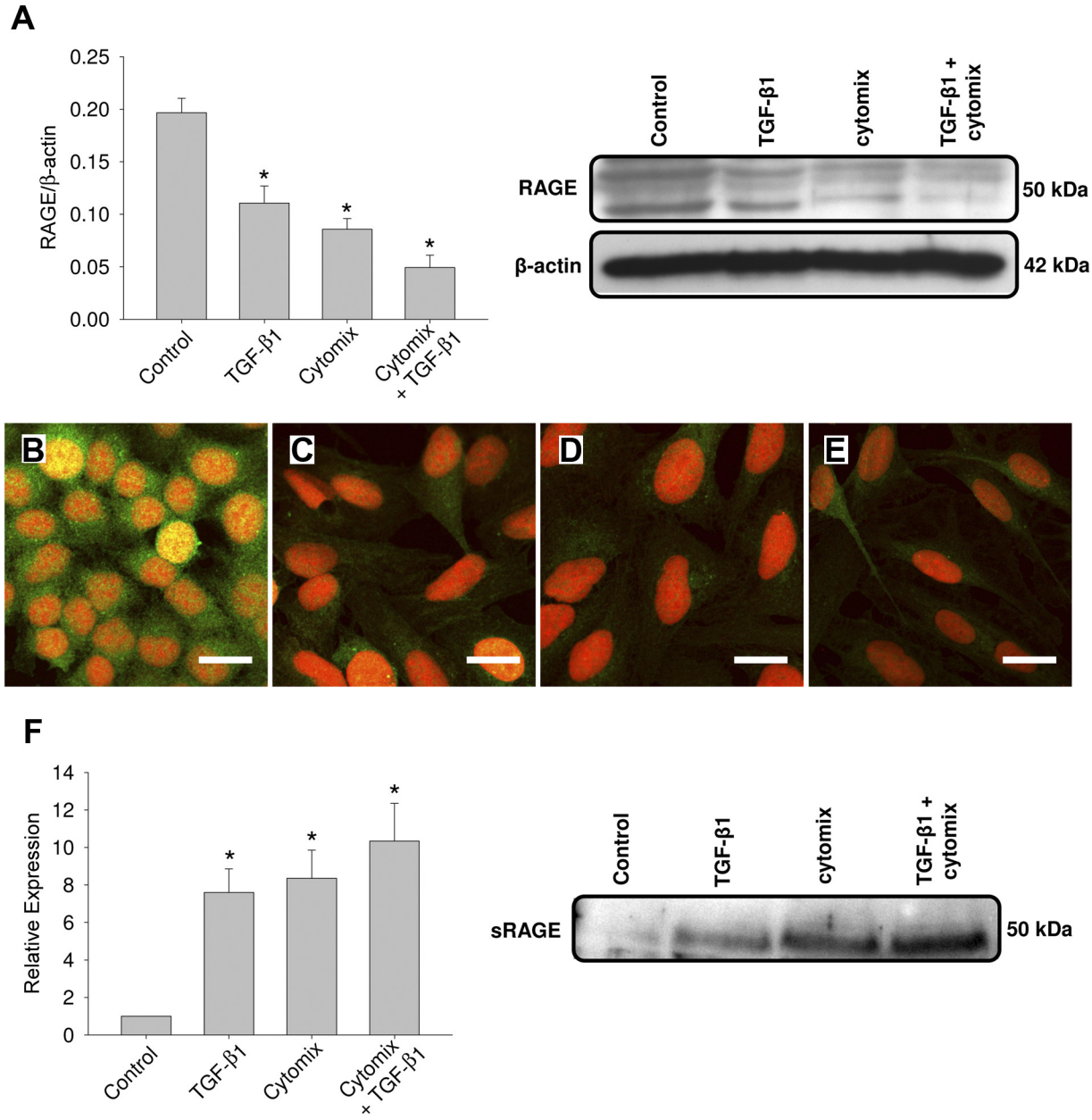

Fig. 3. Downregulation of receptor for advanced glycation end-products (RAGE) and release of soluble RAGE (sRAGE) when treated with TGF-β1 and/or cytomix. *A*: Western blot analysis demonstrated that expression of RAGE in A549 cells was significantly ($P < 0.05$) diminished after treatment with TGF-β1 and/or cytomix for 72 h. *B–E*: immunofluorescence staining for RAGE (green) illustrated that under control conditions cells exhibited diffuse cytoplasmic staining (*B*), which was decreased on cytokine stimulation (TGF-β1, *C*; cytomix, *D*; TGF-β1 + cytomix, *E*). Nuclei were counterstained with propidium iodide (red). *F*: analysis by Western blot of corresponding cell supernatants revealed significantly ($P < 0.05$) enhanced expression of sRAGE in those samples stimulated with TGF-β1 and/or cytomix. Expression levels were evaluated by densitometric analysis and standardized to controls (untreated samples). Means ± SD from >3 independent experiments. *$P < 0.05$. Scale bars are 20 μm.

ings, we observed enhanced MMP-9 expression in treated cells, as shown by CLSM (Fig. 4, *C–F*).

In light of the ability of an inhibitor of MMP-9 to abrogate cytokine-induced sRAGE production and the observed enhanced MMP-9 activity upon cytokine stimulation, we proceeded to investigate the ability of MMP-9 alone to mediate release of sRAGE. As illustrated in Fig. 4*G*, exposure of A549 cells to recombinant MMP-9 (100 ng/ml) gave rise to enhanced levels of sRAGE in the cell supernatant. Moreover, cotreatment with its inhibitor significantly attenuated this effect. Together, these results strongly suggest that MMP-9 contributed to the release of sRAGE into the cell medium.

Uncoupling of RAGE-ERM complex after cytokine stimulation. In untreated A549 cells, RAGE and ERM proteins exhibited marked colocalization, with both showing diffuse cytoplasmic distribution as shown in Fig. 5*A*. Upon treatment with TGF-β1 and/or cytomix, this interaction was uncoupled, with ERM proteins redistributing to the cell membrane and RAGE expression diminishing markedly (Fig. 5, *B–D*). Coimmunoprecipitation analysis confirmed the association of RAGE and ERM proteins in A549 cells (Fig. 5*E*).

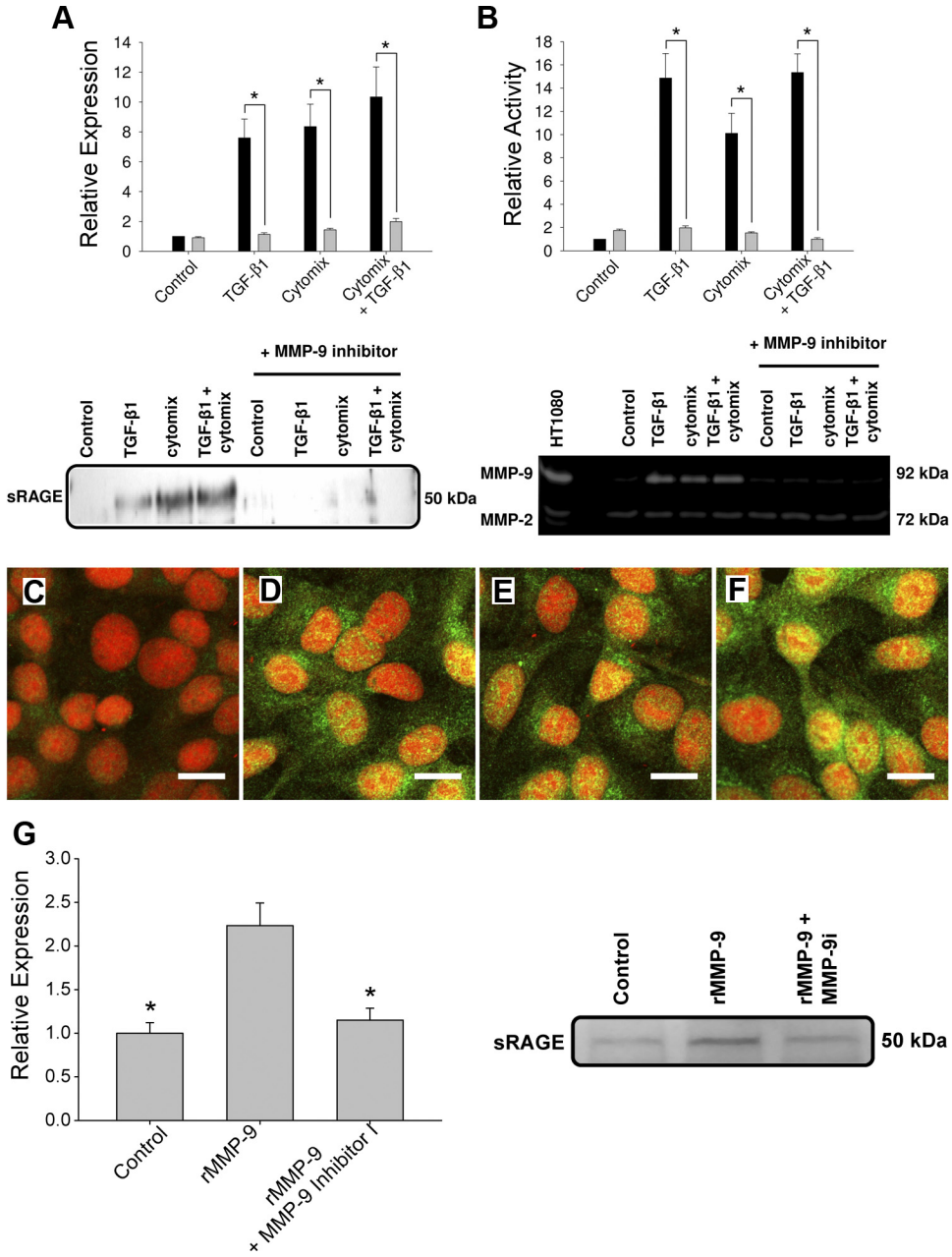

Fig. 4. Matrix metalloproteinase (MMP)-9 mediates release of sRAGE. *A*: when cultures were pretreated with MMP-9 Inhibitor I, cytokine-mediated release of sRAGE into the supernatant was blocked as indicated by Western blot analysis of relevant supernatants. *B*: conditioned medium from untreated A549 cells and from TGF-β1-, cytomix-, or TGF-β1 + cytomix-treated cells was subjected to analysis of gelatinolytic activities by zymography. HT-1080 medium (1st lane) was used as a marker of for pro-MMP-2 and -9. Gelatinases of molecular masses of 72 and 92 kDa corresponding to pro-MMP-2 and pro-MMP-9, respectively, were detected. TGF-β1 and/or cytomix caused significant strong increases in pro-MMP-9 band activities, which was regressed by MMP-9 Inhibitor I (5 nM). Graphs in *A* and *B* depict quantitative analysis of band intensities expressed relative to the control. Black bars, untreated; gray bars, MMP-9 Inhibitor I treated. *C–F*: immunofluorescence staining for MMP-9 (green) revealed enhanced expression levels in stimulated cells. *C*: untreated. *D*: TGF-β1. *E*: cytomix. *F*: TGF-β1 + cytomix. *G*: similarly, exposure to recombinant (r)MMP-9 (100 ng/ml) resulted in increased levels of sRAGE in the cell supernatant, which was ameliorated by pretreatment of cultures with MMP-9 inhibitor I (MMP-9i, 5 nM). Means ± SD from >3 independent experiments. *$P < 0.05$. Bars, 20 μm.

TGF-β1 and proinflammatory cytokines enhance CD44 expression and promote CD44-ERM interaction through phosphorylation of ERM proteins. CD44 is a cellular adhesion receptor that is upregulated after tissue injury, purportedly playing a role in remodeling of pulmonary tissues (20). Moreover, ERM proteins in their active state are known to bind CD44, facilitating their cross-linking with actin filaments (24). Thus we next examined the changes in expression and localization of CD44 in A549 cells by CLSM. In their resting state, A549 cells exhibited weak and diffuse localization of CD44 throughout the cytoplasm (Fig. 6*A*). Upon challenge with TGF-β1 and/or cytomix, enhanced expression of CD44 directly below the plasma membrane was observed (Fig. 6, *B–D*). In agreement with immunofluorescence findings, analysis by Western blot revealed an increase in protein expression of CD44 after treatment, with the effects of both cytomix and TGF-β1 plus cytomix being most marked (Fig. 6*E*).

To examine the relationship between CD44 and ERM, colocalization studies using CLSM were performed, revealing that cytokine treatment induced association of pERM with CD44 (Fig. 6, *F–I*). In particular, strong signals were observed toward the perinuclear region of cells, with more diffuse colocalization noted in cytoplasmic areas. Consistent with CLSM analysis, CD44 was identified in the protein complex immunoprecipitated by anti-pERM antibody, but not by IgG control (Fig. 6*J*).

Expression patterns of RAGE, CD44, and pERM are altered in patient IPF tissues. Dual-fluorescence immunohistochemistry was performed for combinations of RAGE, CD44, and pERM. Representative results are depicted in Fig. 7. In normal

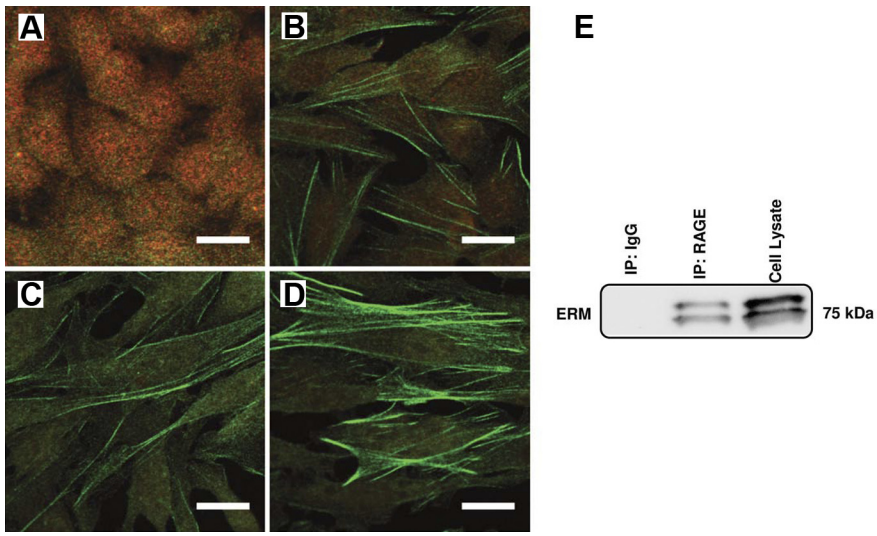

Fig. 5. Cytokine stimulation uncouples ERM-RAGE complex. *A–D*: A549 cells cultured without (*A*) or with TGF-β1 (*B*), cytomix (*C*), or TGF-β1 + cytomix (*D*) for 72 h were subjected to immunofluorescence staining with antibodies to ERM (green) and to RAGE (red). Untreated cells exhibited strong colocalization of ERM and RAGE, with both showing diffuse cytoplasmic distribution. After treatment, this association was disrupted as ERM redistributed toward the cell periphery and RAGE expression was diminished. Bars, 20 μm. *E*: cell lysate from A549 cells was immunoprecipitated (IP) with anti-RAGE antibody or IgG. ERM associated with RAGE was detected by anti-ERM antibody as shown in this representative Western blot. Cell lysate from A549 cells is used as positive control for ERM. All images and blots are representative of at least 3 independent experiments.

lung parenchyma, there was robust expression of RAGE (Fig. 7) that was markedly diminished in fibrotic lesions within IPF tissues. Notably, there was an absence of any double-positive cells for RAGE and pERM in both control and fibrotic lungs (Fig. 7). Also mimicking data obtained in vitro, enhanced expression of CD44 was observed within IPF lung tissue samples. Moreover, distinct populations of double-positive cells for pERM and CD44 as well as for CD44 and RAGE in fibrotic tissues were noted (Fig. 7).

DISCUSSION

There is an ever-growing body of evidence supporting a role for EMT in IPF (17, 21, 40, 43). However, while studies continue to elucidate the underlying pathways of this biological process, the nature of the mechanisms that give rise to the major rearrangements of the submembrane cytoskeleton remain poorly understood. In this study, we assessed the relationship between ERM proteins and RAGE and their functional role in cytokine-induced EMT of an alveolar epithelial cell line, A549.

Members of the ERM family of proteins have previously been shown to be important in regulation of cytoskeletal structure and determination of cellular shape and motility (33, 35, 39, 47). Recently, investigations by Takahashi et al. (38) illustrated that phosphorylation of ERM and subsequent complexation with CD44 was an important step in EMT of retinal pigment epithelial cells, mediating the loss of cell-cell contacts and associated morphological changes. Moreover, in carcinoma-derived renal epithelial cells and pulmonary vascular endothelial cells, cytoskeleton rearrangement was associated with redistribution of members of the ERM family of proteins and their phosphorylation (23, 39). Extending this to the alveolar epithelial setting, our present investigations illustrated that ERM proteins localize toward the cell periphery after cytokine stimulation, entering their activated state and complexing with membrane-associated CD44. Additionally, our studies revealed an interaction between the redistributed ERM proteins and the F-actin stress fibers formed as cells underwent transition to a mesenchymal phenotype, further emphasizing the importance of ERM in determination of cell shape. Collectively, this colocalization is suggestive of a close relationship between cytokine-induced ERM redistribution and phosphorylation and EMT-associated actin remodeling in alveolar epithelial cells.

Several kinases have been implicated in the regulation of ERM protein function. In particular, the Rho-activated kinase ROCK appears to be key in this context (23). Furthermore, the ROCK family are important regulators of actin cytoskeleton organization (29). Notably, in human colonic epithelial cells inhibition of ROCK signaling has been shown to attenuate actin remodeling and prevent ERM phosphorylation, while in migrating intestinal epithelial cells enhanced coassociation of ezrin with CD44 was found to be mediated, in part, by ROCK (16, 33). In light of these findings, we investigated the effect of ROCK inhibition on ERM phosphorylation state. While we did not provide direct evidence for ROCK activation by proinflammatory cytokines, immunoblot analyses revealed that phosphorylation of ERM was blocked by the specific ROCK inhibitor Y-27632. In addition, our investigations revealed that inhibition of ROCK, and thus ERM phosphorylation, contributed toward attenuation of EMT-associated actin stress fiber generation. This implicates ROCK and its downstream effects in the regulation of cytoskeletal structure, and is in agreement with previous findings in epithelia of the lens and kidney (6, 7). We hypothesized that inflammatory cytokines, in particular TGF-β1, induce F-actin stress fibers as a consequence of ROCK activating ERM proteins.

Preservation of an epithelial phenotype and its associated morphological and functional characteristics is crucial to homeostatic maintenance of the alveolar unit. In this regard, RAGE, which is intimately involved in the regulation of adhesion, migration, and proliferation of alveolar epithelial cells (8, 30), exerts an important role. Moreover, pathologically loss of RAGE has been implicated in fibrosis of the pulmonary epithelium (9, 13, 30). In accordance with these observations, we detected a marked decrease in RAGE expression in alveolar epithelial cells after stimulation with TGF-β1 and/or cytomix. Notably, these findings are in contrast to those of He and colleagues (15), who reported that RAGE−/− mice were resistant to bleomycin-induced lung injury, with enhanced survival rates and lower fibrotic scores. Given that RAGE associates with components of the extracellular matrix (ECM)

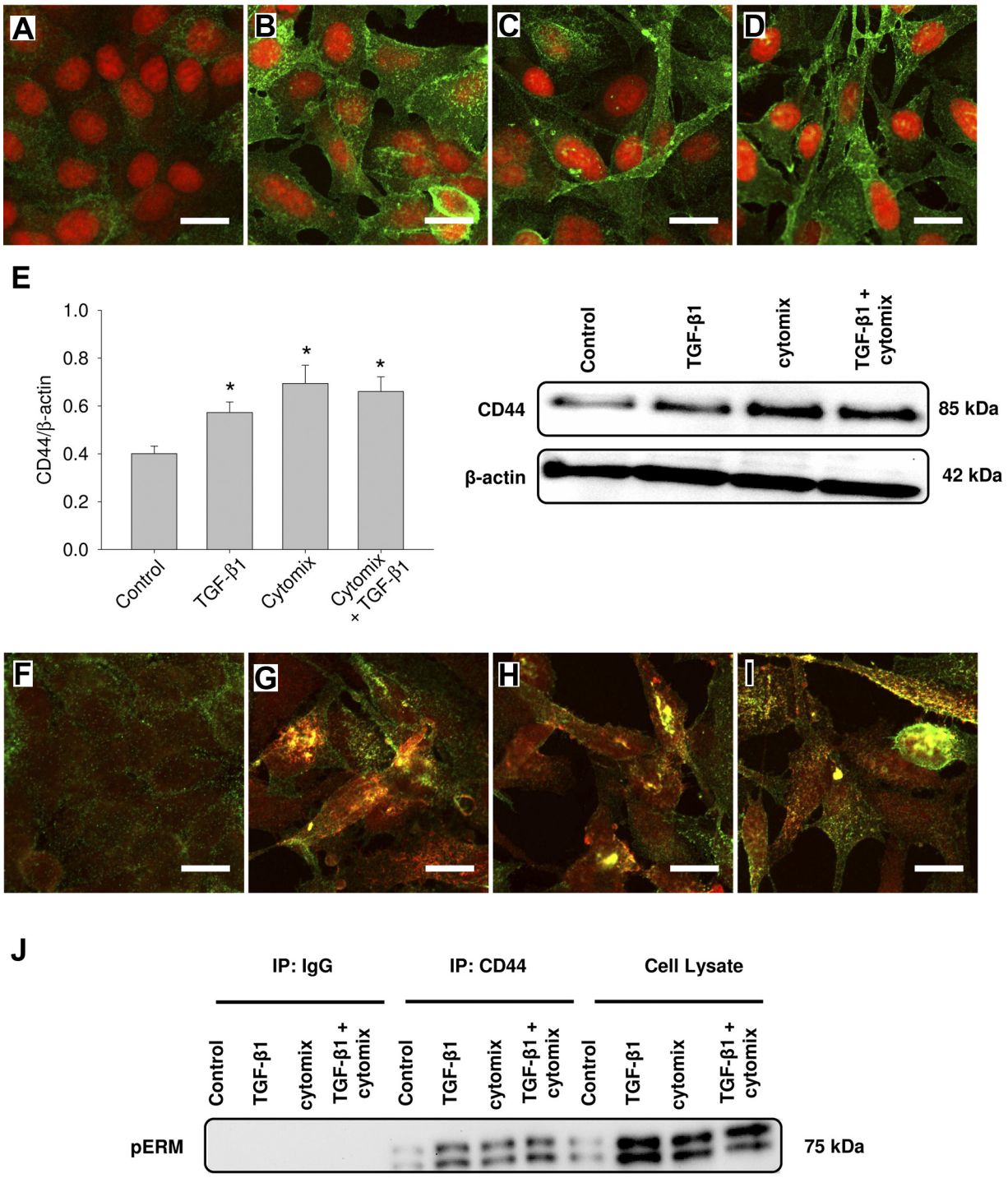

Fig. 6. TGF-β1 and/or cytomix enhance CD44 expression and promote CD44-ERM interaction via phosphorylation of ERM proteins. *A–D*: A549 cells cultured without (*A*) or with TGF-β1 (*B*), cytomix (*C*), or TGF-β1 + cytomix (*D*) for 72 h were subjected to immunofluorescence staining with antibodies to CD44 (green) alone. CLSM analysis revealed increased expression of CD44 directly under the plasma membrane after cytokine treatment. *E*: Western blot analysis demonstrated that expression of CD44 in A549 cells was significantly ($P < 0.05$) enhanced after treatment with TGF-β1 and/or cytomix for 72 h. *F–I*: CLSM colocalization studies were performed for pERM (red) and CD44 (green). *F*: untreated. *G*: TGF-β1. *H*: cytomix. *I*: TGF-β1 + cytomix. Representative images reveal a strong association between pERM and CD44 after cytokine treatment as detailed above. *J*: A549 cells cultured as mentioned above were lysed and subjected to immunoprecipitation with antibodies against CD44 or with control IgG. The resulting precipitates as well as the cell lysates were subjected to immunoblot analysis with antibodies against ERM. The representative blot illustrates a strong association between CD44 and pERM in A549 cells after cytokine stimulation. Means ± SD from >3 independent experiments. *$P < 0.05$. Bars, 20 μm.

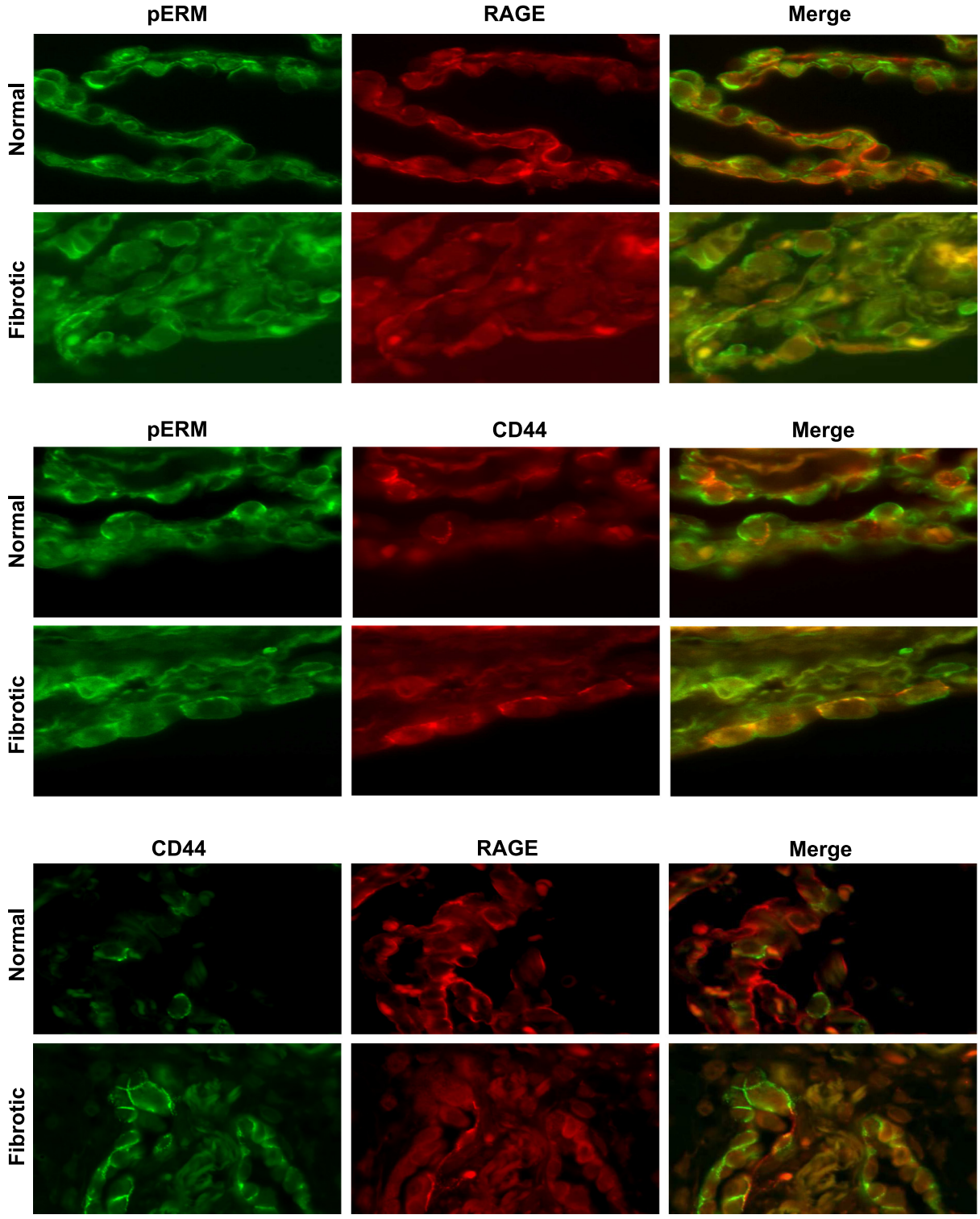

Fig. 7. Altered expression patterns of RAGE, pERM, and CD44 in patient idiopathic pulmonary fibrosis (IPF) tissues. Representative images of dual-fluorescence immunohistochemistry of patient tissues from fibrotic and normal lungs show a noticeable reduction of RAGE in fibrotic tissues and an absence of double-positive cells for RAGE and pERM (*top*). In fibrotic tissues, pERM and CD44 were found to colocalize (*middle*). Increased expression of CD44 in IPF samples was observed and, in addition, coexpression with RAGE in a few alveolar epithelial cells (*bottom*).

(8), conceivably loss of RAGE may lead to diminished affinity for the ECM and in this way increase the susceptibility of epithelial cells of the alveolus to injurious events that propagate the fibrogenic reaction. Given our findings, and that of Queisser and colleagues (30), it appears likely that cytokine-induced RAGE deficiency may be an important component of the EMT process—an acknowledged key contributor to the expanded fibroblast population in IPF.

Next, we investigated the potential mechanism by which RAGE expression levels are diminished. Previous studies have shown that membrane RAGE may be cleaved by proteases to form sRAGE (32, 47) and, in this way, give rise to lower expression of full-length, membrane-bound RAGE. Indeed, in models of acute lung injury (ALI), sRAGE has been found to accumulate in the bronchoalveolar lavage fluid (BALF) (42). Clinical studies have also highlighted the value of sRAGE as a pathogenic and prognostic marker. A strong correlation has been shown to exist between poorer clinical outcomes in patients with ALI and higher baseline plasma sRAGE levels (5), while both air space and perfusate sRAGE levels appear to be negatively correlated with alveolar fluid clearance (2, 11). Similarly, under hyperoxic conditions levels of sRAGE in BALF and lung homogenates have been shown to increase (34, 37). Interestingly, in a bleomycin model of pulmonary fibrosis sRAGE BALF levels were found to decrease after injury (9), while in a silicosis model very little was detected, both before and after injury (31). However, it has been suggested that these conflicting results may be due to rapid clearance of sRAGE following the injurious event. Here, in A549 human alveolar epithelial cells, we observed increased levels of RAGE in the cell supernatant after stimulation with proinflammatory cytokines. The antibody used in this study does not differentiate between sRAGE and the endogenous secretory isoform (esRAGE). Thus a possible contribution by esRAGE cannot be excluded; however, our finding is consistent with the suggestion that increased sRAGE levels are a biological indicator of alveolar epithelial cell injury. MMPs are one of the main proteolytic enzymes involved in tissue remodeling during the fibrotic process. In particular, MMP-9 (gelatinase B) has been shown to mediate the disruption of the alveolar basement membrane (28). Hence, we investigated the effect of inhibition of MMP-9 activity on sRAGE release. Activated MMPs are rarely detected, on account of their fast degradation, and therefore changes in activity of pro-forms were investigated (26). Using gelatin zymography, we verified that stimulation with TGF-β1 and/or cytomix gave rise to enhanced MMP-9 activity. Furthermore, use of an inhibitor of MMP-9 revealed marked abrogation of RAGE release into the cell media of our in vitro model. The important involvement of MMP-9 in RAGE release was underlined by our findings that treatment with recombinant MMP-9 elicited increased levels of RAGE in cell supernatant samples. Together, these results lend support to the hypothesis that proteolysis caused by MMP-9 contributed to sRAGE release into the media, although it is noted that

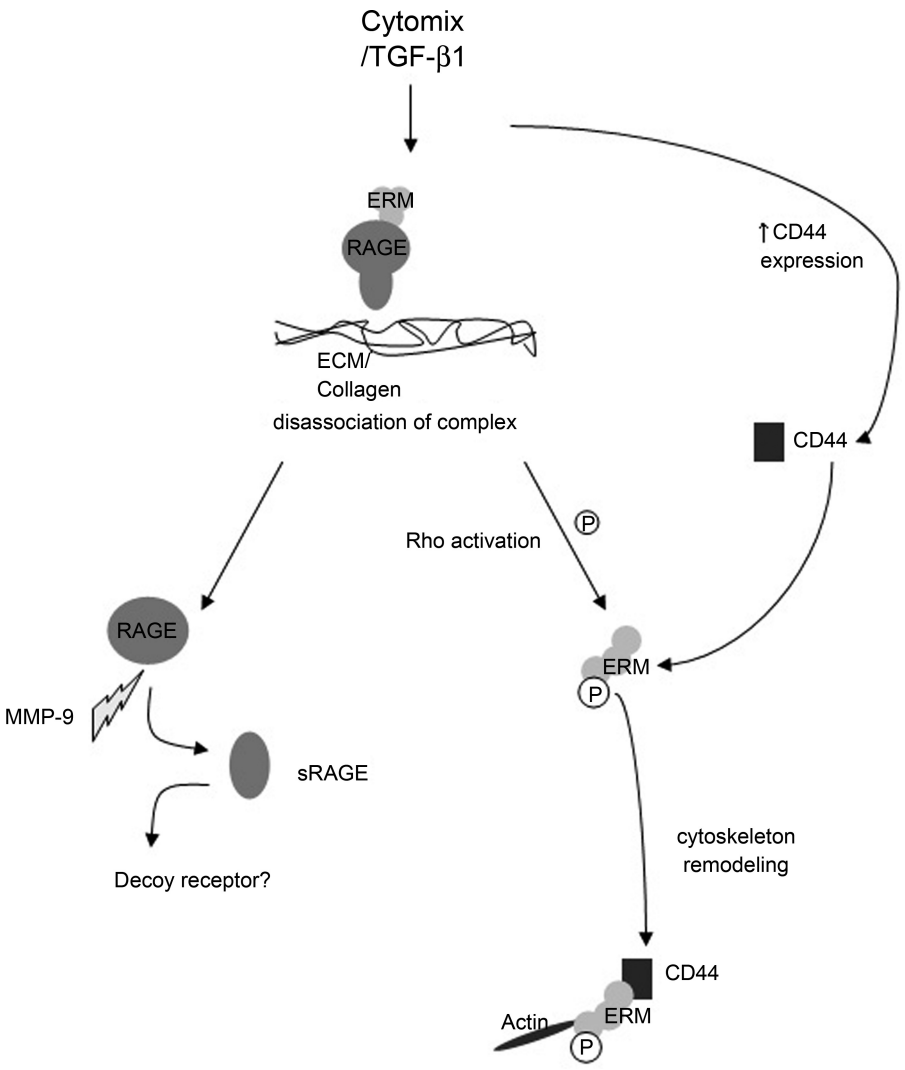

Fig. 8. Proposed schematic of disruption of ERM-RAGE complex in epithelial-mesenchymal transition (EMT) of alveolar epithelial cells. Proinflammatory cytokines induce the expression of CD44, a cellular adhesion receptor involved in pulmonary tissue remodeling, and the phosphorylation of ERM in a manner dependent on ROCK activation. Simultaneously, MMP-9 activity is increased after cytokine stimulation and mediates proteolytic cleavage of RAGE. Collectively, these events serve to promote deterioration of the ERM-RAGE complex. Disruption of this stabilizing complex gives rise to remodeling of the actin cytoskeleton and formation of the ERM-CD44 complex, and ultimately leads to EMT induction.

inhibition of RAGE cleavage did not alter the morphological changes observed in vitro.

Using immunofluorescence confocal microscopy and coimmunoprecipitation, we explored the potential interaction between ERM proteins and RAGE. Interestingly, for the first time, we showed a strong association between the proteins in alveolar epithelial cells under control conditions. Moreover, we found that this complex was disrupted after stimulation with TGF-β1 and/or cytomix, as cells lost their epithelial phenotype and gained characteristics typical of a mesenchymal phenotype, forming stress fibers and adopting a more fibroblast-like appearance. It is important to note that EMT is not a single event; rather, it consists of multiple steps, including epithelial deaggregation, detachment from basement membrane, and cytoskeletal rearrangement (22). Our investigations suggest that disruption of this ERM-RAGE complex is an important component of this process. Conceivably, this event gives rise to a destabilized epithelial state and, in this way, serves to "prime" epithelial cells of the alveolus for transition to a mesenchymal phenotype.

Analysis of patient tissue samples from both healthy and fibrotic lungs lends further credence to our observations in vitro. In accordance with previous findings (9, 30), dual immunohistochemistry studies highlighted a dramatic loss of RAGE in the parenchyma of IPF lung tissue samples. Additionally, we enforced the assertion that CD44 is upregulated in fibrotic pathologies (38) and colocalizes with RAGE in distinct cell populations, which can be speculated to be ATII cells undergoing transdifferentiation either into type I pneumocytes or indeed into mesenchymal cells. We also illustrated an association between CD44 and pERM at injurious sites within the lung parenchyma of biopsy samples of patients with IPF, thus extending our initial observations within A549 cells. In light of these findings in vitro and in vivo, and those of Takahashi and colleagues (38) in retinal pigment epithelial cells, formation of a CD44-pERM complex appears potentially functionally important in the generation of myofibroblasts via EMT.

It is clear from our investigations and those of others (see, e.g., Ref. 43) that epithelia of the alveolus exhibit sufficient plasticity to undergo EMT and that the microenvironment in pulmonary fibrosis is particularly suitable to induce EMT; however, the degree to which this manifests to produce a significant contribution to the fibrotic process requires further investigation. While numerous investigations report alveolar epithelial cells undergoing EMT, both in vitro and in vivo (21, 43), there is a dearth of information detailing the exact proportion of (myo-)fibroblasts in fibrotic pulmonary tissues that are EMT derived. Initial findings suggested that up to 80% of pulmonary epithelial cells coexpressed both epithelial and mesenchymal markers in fibrotic lungs (43). Use of cell-fate mapping models has provided more convincing proof (21). However, evidence remains conflicting. Recent findings by Tanjore and colleagues (40) revealed that although EMT is a source of fibroblasts, it is not a principal contributor to the myofibroblast population, while a separate study failed to find double-positive cells for epithelial markers in tissue samples from either a bleomycin model of fibrosis or one that was human derived (46).

In conclusion, in the present work, we have identified a novel ERM-RAGE complex and shown that disturbance of this complex in a MMP-9- and ROCK-dependent manner can be observed in alveolar EMT. The precise details of our proposed mechanism are depicted in Fig. 8. Our results suggest a potentially important role for both ERM proteins and RAGE in the mechanistic pathway(s) that underpins alveolar EMT, and offer insight into a potential therapeutic target for amelioration of EMT-related fibrosis of the lung. Histochemical evidence suggests that RAGE likely localizes predominantly toward type I alveolar epithelial cells in situ. Although our in vitro study utilized A549 cells, an adenocarcinoma-derived cell line, the extent to which they reflect phenotypic properties specific to type II cells is somewhat restricted (e.g., absence of lamellar bodies). Moreover, previous studies indicate that they are an appropriate model in which to study the biology of RAGE and EMT (19, 30). However, importantly, further experiments are required to confirm these observations in primary cell culture models and to elucidate additional underlying mechanistic details, in particular the exact identity of the member(s) of the ERM family of proteins implicated in the effects observed in our studies.

ACKNOWLEDGMENTS

We are grateful for the technical assistance of S. Bramke and to Dr. K. Kuwano (Jikei University School of Medicine, Tokyo, Japan) for providing the human lung samples.

GRANTS

S. T. Buckley is funded by an Irish Research Council for Science, Engineering & Technology (IRCSET) Government of Ireland Postgraduate Scholarship in Science, Engineering and Technology. C. Medina holds a Science Foundation Ireland (SFI) Stokes Lecturership. This work has been funded in part by a Strategic Research Cluster grant (07/SRC/B1154) under the National Development Plan cofunded by European Union Structural Funds and SFI (C. Ehrhardt).

DISCLOSURES

No conflicts of interest, financial or otherwise, are declared by the author(s).

REFERENCES

1. **Atkinson JJ, Senior RM.** Matrix metalloproteinase-9 in lung remodeling. *Am J Respir Cell Mol Biol* 28: 12–24, 2003.
2. **Briot R, Frank JA, Uchida T, Lee JW, Calfee CS, Matthay MA.** Elevated levels of the receptor for advanced glycation end products, a marker of alveolar epithelial type I cell injury, predict impaired alveolar fluid clearance in isolated perfused human lungs. *Chest* 135: 269–275, 2009.
3. **Buckley ST, Ehrhardt C.** The receptor for advanced glycation end products (RAGE) and the lung. *J Biomed Biotechnol* 2010: 917108, 2010.
4. **Buckley ST, Medina C, Ehrhardt C.** Differential susceptibility to epithelial-mesenchymal transition (EMT) of alveolar, bronchial and intestinal epithelium in vitro. *Cell Tissue Res* 342: 39–51, 2010.
5. **Calfee CS, Budev MM, Matthay MA, Church G, Brady S, Uchida T, Ishizaka A, Lara A, Ranes JL, deCamp MM, Arroliga AC.** Plasma receptor for advanced glycation end-products predicts duration of ICU stay and mechanical ventilation in patients after lung transplantation. *J Heart Lung Transplant* 26: 675–680, 2007.
6. **Cho HJ, Yoo J.** Rho activation is required for transforming growth factor-beta-induced epithelial-mesenchymal transition in lens epithelial cells. *Cell Biol Int* 31: 1225–1230, 2007.
7. **Das S, Becker BN, Hoffmann FM, Mertz JE.** Complete reversal of epithelial to mesenchymal transition requires inhibition of both ZEB expression and the Rho pathway. *BMC Cell Biol* 21: 94, 2009.
8. **Demling N, Ehrhardt C, Kasper M, Laue M, Knels L, Rieber EP.** Promotion of cell adherence and spreading: a novel function of RAGE, the highly selective differentiation marker of human alveolar epithelial type I cells. *Cell Tissue Res* 323: 475–488, 2006.

9. **Englert JM, Hanford LE, Kaminski N, Tobolewski JM, Tan RJ, Fattman CL, Ramsgaard L, Richards TJ, Loutaev I, Nawroth PP, Kasper M, Bierhaus A, Oury TD.** A role for the receptor for advanced glycation end products in idiopathic pulmonary fibrosis. *Am J Pathol* 172: 583–591, 2008.
10. **Fehon RG, McClatchey AI, Bretscher A.** Organizing the cell cortex: the role of ERM proteins. *Nat Rev Mol Cell Biol* 11: 276–287, 2010.
11. **Frank JA, Briot R, Lee JW, Ishizaka A, Uchida T, Matthay MA.** Physiological and biochemical markers of alveolar epithelial barrier dysfunction in perfused human lungs. *Am J Physiol Lung Cell Mol Physiol* 293: L52–L59, 2007.
12. **Gefter JV, Shaufl AL, Fink MP, Delude RL.** Comparison of distinct protein isoforms of the receptor for advanced glycation end-products expressed in murine tissues and cell lines. *Cell Tissue Res* 337: 79–89, 2009.
13. **Hanford LE, Fattman CL, Shaefer LM, Enghild JJ, Valnickova Z, Oury TD.** Regulation of receptor for advanced glycation end products during bleomycin-induced lung injury. *Am J Respir Cell Mol Biol* 29: S77–S81, 2003.
14. **Hashimoto S, Amaya F, Matsuyama H, Ueno H, Kikuchi S, Tanaka M, Watanabe Y, Ebina M, Ishizaka A, Tsukita S, Hashimoto S.** Dysregulation of lung injury and repair in moesin-deficient mice treated with intratracheal bleomycin. *Am J Physiol Lung Cell Mol Physiol* 295: L566–L574, 2008.
15. **He M, Kubo H, Ishizawa K, Hegab AE, Yamamoto Y, Yamamoto H, Yamaya M.** The role of the receptor for advanced glycation end-products in lung fibrosis. *Am J Physiol Lung Cell Mol Physiol* 293: L1427–L1436, 2007.
16. **Hopkins AM, Pineda AA, Winfree LM, Brown GT, Laukoetter MG, Nusrat A.** Organized migration of epithelial cells requires control of adhesion and protrusion through Rho kinase effectors. *Am J Physiol Gastrointest Liver Physiol* 292: G806–G817, 2007.
17. **Jayachandran A, Königshoff M, Yu H, Rupniewska E, Hecker M, Klepetko W, Seeger W, Eickelberg O.** SNAI transcription factors mediate epithelial-mesenchymal transition in lung fibrosis. *Thorax* 64: 1053–1061, 2009.
18. **Kalluri R, Neilson EG.** Epithelial-mesenchymal transition and its implications for fibrosis. *J Clin Invest* 112: 1776–1784, 2003.
19. **Kasai H, Allen JT, Mason RM, Kamimura T, Zhang Z.** TGF-beta1 induces human alveolar epithelial to mesenchymal cell transition (EMT). *Respir Res* 9: 56, 2005.
20. **Kasper M, Haroske G.** Alterations in the alveolar epithelium after injury leading to pulmonary fibrosis. *Histol Histopathol* 11: 463–483, 1996.
21. **Kim KK, Kugler MC, Wolters PJ, Robillard L, Galvez MG, Brumwell AN, Sheppard D, Chapman HA.** Alveolar epithelial cell mesenchymal transition develops in vivo during pulmonary fibrosis and is regulated by the extracellular matrix. *Proc Natl Acad Sci USA* 103: 13180–13185, 2006.
22. **Kim KK, Chapman HA.** Endothelin-1 as initiator of epithelial-mesenchymal transition: potential new role for endothelin-1 during pulmonary fibrosis. *Am J Respir Cell Mol Biol* 37: 1–2, 2007.
23. **Koss M, Pfeiffer GR 2nd, Wang Y, Thomas ST, Yerukhimovich M, Gaarde WA, Doerschuk CM, Wang Q.** Ezrin/radixin/moesin proteins are phosphorylated by TNF-alpha and modulate permeability increases in human pulmonary microvascular endothelial cells. *J Immunol* 176: 1218–1227, 2006.
24. **Louvet-Vallée S.** ERM proteins: from cellular architecture to cell signaling. *Biol Cell* 92: 305–316, 2000.
25. **McCawley LJ, Matrisian LM.** Matrix metalloproteinases: they're not just for matrix anymore! *Curr Opin Cell Biol* 13: 534–540, 2001.
26. **Medina C, Videla S, Radomski A, Radomski MW, Antolin M, Guarner F, Vilaseca J, Salas A, Malagelada JM.** Increased activity of matrix metalloproteinase-9 in a rat model of distal colitis. *Am J Physiol Gastrointest Liver Physiol* 284: G116–G122, 2003.
27. **Neeper M, Schmidt AM, Brett J, Yan SD, Wang F, Pan YC, Elliston K, Stern D, Shaw A.** Cloning and expression of a cell surface receptor for advanced glycosylation end products of proteins. *J Biol Chem* 267: 14998–15004, 1992.
28. **Pardo A, Selman M.** Matrix metalloproteases in aberrant fibrotic tissue remodeling. *Proc Am Thorac Soc* 3: 383–388, 2006.
29. **Pellegrin S, Mellor H.** Actin stress fibres. *J Cell Sci* 120: 3491–3499, 2007.
30. **Queisser MA, Kouri FM, Königshoff M, Wygrecka M, Schubert U, Eickelberg O, Preissner KT.** Loss of RAGE in pulmonary fibrosis: molecular relations to functional changes in pulmonary cell types. *Am J Respir Cell Mol Biol* 39: 337–345, 2008.
31. **Ramsgaard L, Englert JM, Tobolewski J, Tomai L, Fattman CL, Leme AS, Kaynar AM, Shapiro SD, Enghild JJ, Oury TD.** The role of the receptor for advanced glycation end-products in a murine model of silicosis. *PLoS One* 5: e9604, 2010.
32. **Raucci A, Cugusi S, Antonelli A, Barabino SM, Monti L, Bierhaus A, Reiss K, Saftig P, Bianchi ME.** A soluble form of the receptor for advanced glycation endproducts (RAGE) is produced by proteolytic cleavage of the membrane-bound form by the sheddase a disintegrin and metalloprotease 10 (ADAM10). *FASEB J* 22: 3716–3727, 2008.
33. **Rebillard A, Jouan-Lanhouet S, Jouan E, Legembre P, Pizon M, Sergent O, Gilot D, Tekpli X, Lagadic-Gossmann D, Dimanche-Boitrel MT.** Cisplatin-induced apoptosis involves a Fas-ROCK-ezrin-dependent actin remodelling in human colon cancer cells. *Eur J Cancer* 46: 1445–1455, 2010.
34. **Reynolds PR, Schmitt RE, Kasteler SD, Sturrock A, Sanders K, Bierhaus A, Nawroth PP, Paine R 3rd, Hoidal JR.** Receptors for advanced glycation end-products targeting protect against hyperoxia-induced lung injury in mice. *Am J Respir Cell Mol Biol* 42: 545–551, 2010.
35. **Rollason R, Korolchuk V, Hamilton C, Jepson M, Banting G.** A CD317/tetherin-RICH2 complex plays a critical role in the organization of the subapical actin cytoskeleton in polarized epithelial cells. *J Cell Biol* 184: 721–736, 2009.
36. **Speck O, Hughes SC, Noren NK, Kulikauskas RM, Fehon RG.** Moesin functions antagonistically to the Rho pathway to maintain epithelial integrity. *Nature* 421: 83–87, 2003.
37. **Su X, Looney MR, Gupta N, Matthay MA.** Receptor for advanced glycation end-products (RAGE) is an indicator of direct lung injury in models of experimental lung injury. *Am J Physiol Lung Cell Mol Physiol* 297: L1–L5, 2009.
38. **Takahashi E, Nagano O, Ishimoto T, Yae T, Suzuki Y, Shinoda T, Nakamura S, Niwa S, Ikeda S, Koga H, Tanihara H, Saya H.** Tumor necrosis factor-alpha regulates transforming growth factor-beta-dependent epithelial-mesenchymal transition by promoting hyaluronan-CD44-moesin interaction. *J Biol Chem* 285: 4060–4073, 2010.
39. **Takenouchi H, Kiyokawa N, Taguchi T, Matsui J, Katagiri YU, Okita H, Okuda K, Fujimoto J.** Shiga toxin binding to globotriaosyl ceramide induces intracellular signals that mediate cytoskeleton remodeling in human renal carcinoma-derived cells. *J Cell Sci* 117: 3911–3922, 2004.
40. **Tanjore H, Xu XC, Polosukhin VV, Degryse AL, Li B, Han W, Sherrill TP, Plieth D, Neilson EG, Blackwell TS, Lawson WE.** Contribution of epithelial-derived fibroblasts to bleomycin-induced lung fibrosis. *Am J Respir Crit Care Med* 180: 657–665, 2009.
41. **Thannickal VJ, Toews GB, White ES, Lynch JP 3rd, Martinez FJ.** Mechanisms of pulmonary fibrosis. *Annu Rev Med* 55: 395–417, 2004.
42. **Uchida T, Shirasawa M, Ware LB, Kojima K, Hata Y, Makita K, Mednick G, Matthay ZA, Matthay MA.** Receptor for advanced glycation end-products is a marker of type I cell injury in acute lung injury. *Am J Respir Crit Care Med* 173: 1008–1015, 2006.
43. **Willis BC, Liebler JM, Luby-Phelps K, Nicholson AG, Crandall ED, du Bois RM, Borok Z.** Induction of epithelial-mesenchymal transition in alveolar epithelial cells by transforming growth factor-beta1: potential role in idiopathic pulmonary fibrosis. *Am J Pathol* 166: 1321–1332, 2005.
44. **Willis BC, duBois RM, Borok Z.** Epithelial origin of myofibroblasts during fibrosis in the lung. *Proc Am Thorac Soc* 3: 377–382, 2006.
45. **Willis BC, Borok Z.** TGF-beta-induced EMT: mechanisms and implications for fibrotic lung disease. *Am J Physiol Lung Cell Mol Physiol* 293: L525–L534, 2007.
46. **Yamada M, Kuwano K, Maeyama T, Hamada N, Yoshimi M, Nakanishi Y, Kasper M.** Dual-immunohistochemistry provides little evidence for epithelial-mesenchymal transition in pulmonary fibrosis. *Histochem Cell Biol* 129: 453–462, 2008.
47. **Zhang L, Bukulin M, Kojro E, Roth A, Metz VV, Fahrenholz F, Nawroth PP, Bierhaus A, Postina R.** Receptor for advanced glycation end products is subjected to protein ectodomain shedding by metalloproteinases. *J Biol Chem* 283: 35507–35516, 2008.